Multiple levels of stochasticity accounted for in different radiation biophysical models: from physics to biology

Francesco G. Cordoni [1,2,*], Marta Missiaggia [2,3,4],

Chiara La Tessa[2,3] and Emanuele Scifoni[2]

1 University of Trento, Department of Civil, Environmental and Mechanical Engineering, Trento, Italy.

2 TIFPA-INFN, Trento, Italy.

3 University of Trento, Department of Physics, Trento, Italy.

4 Museo Storico della Fisica e Centro Studi e Ricerche Enrico Fermi, Rome, Italy.

* Corresponding author; email: francesco.cordoni@unitn.it

Keywords or phrases: Stochastic radiobiological models, cell survival assessment, microdosimetry, radiation biophysical modeling.

Abstract

Purpose: in the present paper we investigate how some stochastic effects are included in a class of radiobiological models with particular emphasis on how such randomnesses reflect into the predicted cell survival curve.

Materials and Methods: we consider four different models, namely the *Generalized Stochastic Microdosimetric Model* GSM^2 , in its original full form, the *Dirac* GSM^2, the *Poisson* GSM^2 and the *Repair-Misrepair Model* (RMR). While GSM^2 and the RMR models are known in literature, the Dirac and the Poisson GSM^2 have been newly introduced in this work. We further numerically investigate via Monte Carlo simulation of four different particle beams, how the proposed stochastic approximations reflect into the predicted survival curves. To achieve these results, we consider different ion species at energies of interest for therapeutic applications, also including a mixed field scenario.

Results: we show how the *Dirac* GSM^2, the *Poisson* GSM^2 and the RMR can be obtained from the GSM^2 under suitable approximations on the stochasticity considered. We analytically derive the cell survival curve predicted by the four models, characterizing rigorously the high and low dose limits. We further study how the theoretical findings emerge also using Monte Carlo numerical simulations.

Conclusions: we show how different models include different levels of stochasticity in the description of cellular response to radiation. This translates into different cell survival predictions depending on the radiation quality.

Introduction

The last decades have seen increasing attention to the development of mathematical models to describe the biological damage due to irradiation of different types. The main applications of such models are radiotherapy and space radioprotection. Although a

plethora of mathematical models has been proposed over the years (Albright 1989; Bellinzona et al. 2021; Curtis 1986; Thomas Friedrich et al. 2012; Hawkins 1994, 2003, 2018; Inaniwa et al. 2013; Kase et al. 2006; Kellerer and Rossi 1978; McMahon 2018; Nomiya 2013; Rossi and Zaider 1988; Sato and Furusawa 2012; Scholz et al. 1997; Tobias 1980, 1985; Vassiliev 2012; Zhao et al. 2015, 2015; Zhao, Mi, and Sun 2017), providing several mechanistic insights and successful predictive power in some cases, a rigorous analysis of the probabilistic setting of the model themselves is often missing. In particular, special attention on the assumed probability distributions for the driving processes and how much they reflect into the prediction of the cell–survival curves, is of interest to understand the range of validity of each model.

In (Cordoni, Missiaggia, Attili, et al. 2021), the *Generalized Stochastic Microdosimetric Model* (GSM^2) has been formally introduced, which aims at deriving a general probabilistic framework to treat DNA-damage formation and kinetics and a differential equation for the time–evolution of the probability distribution of DNA damage. GSM^2 is in fact a fully probabilistic model whose goal is to accurately describe the stochastic nature of energy deposition in volumes of interest for cellular systems. The final objective of GSM^2 is to overcome the main limitations of existing models, which most assume a Poisson density for damages induced by ionizing radiation, to provide a better prediction of biological endpoints relevant for radiotherapy applications. In complete generality, it has been shown how the stochastic nature of energy deposition and a suitable probabilistic description of the damage kinetics can be used to obtain a *master equation* describing the spatio–temporal damage density function. It is further described in (Cordoni, Missiaggia, Scifoni, et al. 2022) how different parameters, initial DNA damage distribution or irradiation

conditions can lead naturally to several possible probability distributions that can be significantly different from the typically assumed Poissonian law. Thus, in (Cordoni, Missiaggia, Scifoni, et al. 2022; Missiaggia, Cordoni, et al. 2021), a detailed treatment of the survival fraction curve predicted by GSM^2 has been carried out, studying the theoretical properties of its behavior and validating it with Monte Carlo simulations. The current work proceeds with the systematic investigation of the stochastic effects inherent to energy deposition started in (Cordoni, Missiaggia, Attili, et al. 2021; Cordoni, Missiaggia, Scifoni, et al. 2022; Missiaggia, Cordoni, et al. 2021).

It is, however, worth stressing that, a relevant limitation shared by most of the mathematical models and by GSM^2, is a spatial ideal homogeneity. It is in fact assumed for computational reasons that the probability that a pair of DSBs undergoes a certain process is independent of the initial distance between the DSBs. Regarding GSM^2, although the mathematical formalism can in principle include information on energy deposition and radiation quality at the micrometer scale, as well as relevant deviations from a purely Poissonian distribution on the number of DNA damages induced, it requires that damage processing should be homogeneous throughout the domain considered, neglecting thus the real distance between DSBs. At the same time, there is clear evidence that track structure at the nano and micrometer scale is extremely relevant to DSB processing. For these reasons, over the years numerous track structure codes have been developed, (Bernal et al. 2015; Brenner 1990; Charlton, DE and Nikjoo, H and Humm, JL 1989.; Dingfelder 2012; Friedland et al. 2011; Goodhead, DT and Leenhouts, HP and Paretzke, HG and Terrissol, M and Nikjoo, H and Blaauboer, R 1994.; Incerti et al. 2016, 2018; Kyriakou et al. 2017, 2021; Nikjoo H., S. Uehara W.E. Wilson M. Hoshi M. D.T. Goodhead. 1998; Paretzke, Herwig G 1987; Plante

2011; Plante, Poignant, and Slaba 2021; Schuemann et al. 2019; Wälzlein et al. 2014; Zaider, M and Brenner, DJ and Wilson, WE 1983), to describe physical deposition inside the nucleus at the nano and micron scale.

In previous works, (Cordoni, Missiaggia, Attili, et al. 2021; Cordoni, Missiaggia, Scifoni, et al. 2021; Missiaggia, Cordoni, et al. 2021), it has been often noted how GSM^2, despite its more general probabilistic framework, shares several aspects and analogies with existing radiobiological models. Therefore, broadly speaking, GSM^2 can be interpreted as a suitable generalization of some existing models to account for several levels of stochastic effects relevant to energy deposition and damage induced by ionizing radiation.

In particular, (Cordoni, Missiaggia, Attili, et al. 2021) proves how the main equation of the GSM^2, named *Microdosimetric Master Equation* (MME), can be linked, under a specific Poissonian assumption, to the main equations of the *Repair-misrepair* (RMR) model, (Tobias 1980, 1985). The RMR is a purely Poissonian model that has been developed to interpret radiobiological experiments with heavy ions. The present paper is devoted to deepening some insights made in previous publications, (Cordoni, Missiaggia, Attili, et al. 2021; Cordoni, Missiaggia, Scifoni, et al. 2022), to establish a clear connection between GSM^2 and RMR, with particular attention to the cell survival curve predicted and ~~on~~ its dependence on radiation quality and biological parameters.

Besides GSM^2 and the RMR, two other models will be here newly introduced and studied. Such models place themselves in between RMR and the GSM^2 in terms of generality from a purely probabilistic point of view, thus providing a theoretical link between them. The first model considered, called in the current work *Poisson* GSM^2, is governed by the MME

introduced in (Cordoni, Missiaggia, Attili, et al. 2021) equipped with a Poisson initial law. In this sense, as commented in (Cordoni, Missiaggia, Scifoni, et al. 2022), it can be seen that for low LET radiation, GSM^2 initial DNA damage assessment closely recovers Poissonian behavior.

The other new model considered, named *Dirac GSM*^{2} , is a probabilistic model based on GSM^2 with a specific assumption on the energy deposition described by microdosimetry. Such assumption replaces the microdosimetric energy spectra by their average value z_F; in doing so the Dirac GSM^2 neglects energy deposition fluctuations. The Dirac GSM^2 is computationally less complex than the GSM^2 so it can be regarded as fast implementation of the GSM^2 . It is worth stressing that such microdosimetric approximation, to the best of our knowledge, has been first considered in the early work, (Albright 1989). The resulting DNA damage distribution is a known probability distribution studied under a purely mathematical point of view in (Neyman 1939), and more recently it has been used as the main distribution in a *Multi-hit model* (MH), (Vassiliev 2012, 2017).

The aim of the present research is to study the range of validity of different probabilistic assumptions and how this is reflected in the survival curve shape predicted by the models. Such a study will also highlight how different stochastic effects are naturally embedded in the original formulation of GSM^2 . Such terms are usually referred to in the literature as non-Poissonian effects since they are non-linear terms that concur to deviate the true underlying probability distribution from the Poisson random variable. We will therefore show how such non-Poissonianity in the number of DNA damages, may arise either at the

DNA damage formation level or also due to cluster effects in the kinetics and repair of lesions.

The present work therefore analytically studies the survival curve predicted by the four above-mentioned models, i.e., RMR, Poisson GSM^2, Dirac GSM^2, and GSM^2 , characterizing the asymptotic behaviors of the log-survival at both low and high dose limits. We will thus analyze and compare the high and low dose limit, studying similarities and differences as well as their dependence on either biological or radiation quality parameters. Thus, we will further investigate the relevance of the differences in the models emphasized by the theoretical results using Monte Carlo simulations of different ions of therapeutic interest.

It is worth stressing that, although the paper has a purely theoretical flavor, we believe that points raised in the present work can be significant to improving the knowledge of the community on the effect of ionizing radiation on biological tissue, with in turn an impact on radiotherapy. In fact, a robust understanding of DNA-damages kinetics and repair can improve radiotherapy treatment, e.g. in out-of-field regions, where healthy tissue necessarily receives unwanted doses or also heavy ion treatments. Both these situations are dominated by a number of relevant stochastic effects, which must be well described and predicted by a biophysical model in order to deliver the best possible radiotherapy treatment for maximum tumor control while minimizing the occurrence of side effects.

At last, it is worth explicitly mentioning that one of the most relevant radiobiological models that exhibits a clear connection to GSM^2 , namely the *Microdosimetric Kinetic Model* (MKM), and its following generalizations, (Bellinzona et al. 2021; Hawkins 1994, 2003, 2018; Inaniwa et al. 2013; Kase et al. 2006; Sato and Furusawa 2012), have not been

included into the current work. This is due to the fact that, although GSM^2 is clearly inspired by the aforementioned work, there is a typical assumption made in all of the above works that it is not made in GSM^2 . In particular, the MKM assumes that $bx^2 \ll (a+r)x, see\ below\ for\ details$. This simple assumption has the immediate consequence that parameters used in the MKM cannot be directly compared to the ones used in GSM^2 at the level of the kinetic equations whereas the original idea of the work was to give a theoretical comparison of some models whose parameters have the same meaning. This would lead to an exact understanding of how certain assumptions reflects in the predicted cell survival curve, given the exact same parameters. Including the MKM would necessarily imply dropping the parallelism between used parameters and turning to an empirical comparison of the models. Nonetheless, a deep analysis of the similarities and differences between GSM^2 and the MKM is currently under dedicated investigation and, given its extreme relevance, it will the object of future research.

Theory and calculations

The Generalized Stochastic Microdosimetric Model

GSM^2 has been first introduced in (Cordoni, Missiaggia, Attili, et al. 2021), where a detailed description of the model structure can be found. The model is based on the following founding assumptions:

1. the cell nucleus can be divided into N_d independent domains d;

2. radiation can create two different types of DNA damages, called lethal and sublethal lesions;

3. lethal lesions represent a damage that cannot be repaired, while sublethal lesions can be either repaired or converted into a lethal lesion either by spontaneous dead or by combining with another sublethal lesion;

4. the number of lethal and sublethal lesions in a single domain d is proportional to the specific energy z deposited by radiation on the domain.

The further assumptions are then made to decide the cell fate:

5. if at least one domain suffers a lethal lesion, then it is considered dead;

6. if at least one domain is dead, then the whole cell is dead.

Remark 1. Regarding point 4 in previous assumptions, it is worth mentioning that, although in the previous works (Cordoni, Missiaggia, Attili, et al. 2021; Cordoni, Missiaggia, Scifoni, et al. 2022) the constant κ of the average yield per Gy has been assumed to be independent of the radiation quality, in the present paper we will include an enhancement of the average number of lesion yield per unit Gy depending on the radiation quality, as introduced in (Chen et al. 2017; Wang et al. 2018). Such GSM^2 will be explained in more details later in the paper.

A comment on this point is necessary. In fact, correctly estimating the initial number of DNA damages induced by radiation is by far not an easy task. Several approaches are possible, such as fitting the parameter from MC simulations, (Wang et al. 2018). In order to maintain analytical tractability, most of the mathematical models assumes a linear

dependence on the dose of the average DNA damages yields, which is independent on the radiation quality. The independence on the average number of damages induced and the radiation quality is however not true, as shown by several works, (Chen et al. 2017; Wang et al. 2018). For these reasons, *ad hoc* corrections are typically added to account for the variability as a function of the radiation quality of the number of induced damages, as done for instance in (T Friedrich, Durante, and Scholz 2015) within the context of the *Local Effect Model* (LEM) or in (Chen et al. 2017) within the context of the MKM. Ongoing research is currently under study to generalize GSM^2 to include radiation quality dependent average damage yield, generalizing thus the linear dependence on the average damage yield per Gy.

Using this description, lethal lesions represent clustered DNA damage that cannot be repaired whereas sublethal lesions are double-strand breaks that can be repaired. Since the final goal of the present research is to compare the survival curve resulting from the GSM^2 to the survival curve predicted by the RMR and by two newly introduced radiobiological models obtained introducing certain assumptions on the initial damage distribution, we will consider the trivial case of a single domain equal to the nucleus size. This is due to two main reasons: on one side both the RMR and the MH model are formulated without any domain division of the cell nucleus and on the other side we focus solely on the shape of the predicted survival curve without any inter-cellular corrections. On this last point, it is clear that inter-cellular corrections and domain division increase the predicting power of GSM^2, but results contained in the present paper show that major differences in the stochastic formulation of above-mentioned models already emerge at the domain level.

It is worth stressing that, although GSM^2 includes several relevant stochasticity levels in the radiation induced DNA damages formation and kinetics, some limitations are still present. Among the most relevant we mention a spatial homogeneity within the domain at both biological levels, in the sense that the distance between DSBs is not explicitly included into GSM^2, and at physical level, in the sense that a track-structure of energy deposition accounting for track length stochasticity, delta-rays and spatial correlation between tracks is not accounted in GSM^2 . The choice on the GSM^2 assumptions have been clearly done to have a good compromise to a fairly general stochastic model and to maintain a reasonable computational time. Nonetheless, research is currently ongoing to generalize GSM^2 dropping these assumptions. In this direction in fact, a novel detector based on an augmented microdosimetric information has been proposed in, (Missiaggia, Pierobon, et al. 2021), with the final goal to experimentally measure the microdosimetric track length of particles traversing the region of interest. Such information of track stochasticity can help in establishing a more meaningful connection between energy deposition and DNA damage formation.

Aiming therefore at modelling the time–evolution of the number of type lethal and sub–lethal lesion, we will denote by $\big(Y(t), X(t)\big)$ the state of the system at time t, where X and Y are two $\mathbb{N}$ −valued random variables counting the number of lethal and sub–lethal lesions, respectively.

Let us consider two different sets $\mathcal{X}$ and $\mathcal{Y}$ denoting respectively the number of lethal and sublethal lesions, while $\mathcal{A}$ is the set that accounts to healthy cells. We assume that a sublethal lesion becomes a lethal lesion at rate a and recovers at rate r, going back to the

set $\mathcal{A}$, whereas b is the rate at which two sublethal lesion interact with each other to become a lethal lesion.

Above reasoning can be represented as follows

$$\begin{aligned} &X \xrightarrow{a} Y\,, \\ &X \xrightarrow{r} A\,, \\ &X + X \xrightarrow{b} Y\,. \end{aligned} \qquad (1)$$

Defining the probability to observe, at a given time $t > 0$, x sub-lethal lesions and y lethal lesions

$$p(t, y, x) = \mathbb{P}\Big(\big(Y(t), X(t)\big) = (y, x)\Big).$$

we have that $p(t, y, x)$ solves the *Microdosimetric Master Equation* (MME), (Cordoni, Missiaggia, Attili, et al. 2021),

$$\begin{aligned} \partial_t p(t, y, x) \quad &= \mathcal{E}^{-1,2}[x(x-1)bp(t, y, x)] + \\ &+\mathcal{E}^{-1,1}[xap(t, y, x)] + \mathcal{E}^{0,1}[xrp(t, y, x)]\,, \end{aligned} \qquad (2)$$

where above we have denoted the creation operators defined as

$$\mathcal{E}^{i,j}[p(t, y, x)] := p(t, y + i, x + j) - p(t, y, x)\,.$$

The MME (2) is coupled with an initial damage distribution. Such distribution can be obtained from microdosimetric spectra as follows.

Let $f_1(z)$ be the single–event distribution of energy deposition on a domain d, (Zaider, Rossi, and Zaider 1996). The single–event distribution f_1 can be either computed numerically via a Monte Carlo toolkit or retrieved by experimental microdosimetric measurements.

The probability distribution of an energy deposition on a single domain depends on the number of events that deposit energy on the cell nucleus. Given a cell nucleus domain d the probability that ν events deposit an energy z obeys to a Poissonian distribution of mean $\lambda_n := \frac{D}{z_F}$, being D the mean energy deposition on the nucleus and z_F the first moment of the single event distribution f_1. Then, assuming a Poissonian probability that a domain register ν events, the energy deposition distribution is given by

$$f_n(z|D) := \sum_{\nu=0}^{\infty} \frac{e^{-\frac{D}{z_F}}}{\nu!} \left(\frac{D}{z_F}\right)^{\nu} f_\nu(z)\,, \quad (3)$$

where $f_{\nu;d}(z)$ is the energy deposition distribution resulting from ν depositions.

In particular, the distribution resulting from ν events can be computed convolving ν times the single event distribution, see, (Zaider, Rossi, and Zaider 1996). Therefore, the imparted energy z has distribution $f_{\nu;d}$, computed iteratively as

$$\begin{aligned} f_2(z) &:= \int_0^{\infty} f_1(\bar{z}) f_1(z-\bar{z}) d\bar{z}\,, \\ &\dots\,, \\ f_\nu(z) &:= \int_0^{\infty} f_1(\bar{z}) f_{\nu-1}(z-\bar{z}) d\bar{z}\,. \end{aligned}$$

Given an energy deposition z, the induced number of lesions is again a random variable. The standard assumption is that the distribution of sublethal lesions X given z, is a Poisson random variable of mean value κz. Analogous reasoning holds for Y, being the number of induced lethal lesions given z, a Poisson random variable of mean λz.

Putting all the above reasoning together, the MME (2) becomes

$$\begin{cases} \partial_t p(t,y,x) & = \mathcal{E}^{-1,2}[x(x-1)bp(t,y,x)] + \\ & +\mathcal{E}^{-1,1}[xap(t,y,x)] + \mathcal{E}^{0,1}[xrp(t,y,x)] \,, \\ p(0,y,x) & = p_0^X(x)p_0^Y(y) \,, \end{cases} \quad (4)$$

where the initial distribution is obtained as

$$\begin{aligned} p_0^X(x) &= \int_0^\infty p_z^X(x|\kappa z) f(z|D) dz \,, \\ p_0^Y(y) &= \int_0^\infty p_z^Y(y|\lambda z) f(z|D) dz \,. \end{aligned} \quad (5)$$

The initial condition (5) represents a simple and yet important generalization of the standard assumptions, and it must be stressed that both p_0^X and p_0^Y may fail to be Poissonian distributed even if $p_z^X(x|\kappa z)$ and $p_z^Y(y|\lambda z)$ are Poisson random variables. In fact, in (Cordoni, Missiaggia, Scifoni, et al. 2022), it has been shown how, even in the case $p_z^X(x|\kappa z)$ to be a Poisson random variable, the initial distribution $p_0^X(x)$ does not need to be Poissonian. The details of the calculations, not repeated here, are reported in Appendix A.1 or also available for the interested reader in (Cordoni, Missiaggia, Scifoni, et al. 2022; Missiaggia, Cordoni, et al. 2021).

As mentioned above, for the sake of simplicity, in the present work we will assume that no initial lethal lesions can be made. In particular, we will consider $\lambda = 0$, so that $p_0^Y(y) \equiv 0$. Although the number of initial lethal lesions plays a key role in the damage formation, the previous choice of $\lambda = 0$ is made to focus on sub-lethal lesion formation and evolution and on its stochastic effects, without any additional terms. Further, the addition of initial lethal damage, from a mathematical point of view, would be a linear term, (Cordoni, Missiaggia, Scifoni, et al. 2022), that typically follows a Poisson distribution since $\lambda \ll 1$.

In (Cordoni, Missiaggia, Scifoni, et al. 2022) it has been shown that the cell-survival curve for the GSM^2 as developed in (Cordoni, Missiaggia, Attili, et al. 2021) can be explicitly computed as

$$S(D) = p_0^X(0|D) + \frac{r}{a+r} p_0^X(1|D) + \sum_{x_0=2}^{\infty} p_0^X(x_0|D) C(x_0)\,, \quad (7)$$

with

$$C(x_0) := \frac{r^{x_0} x_0!}{\gamma(1) \dots \gamma(x_0)}\,, \quad \gamma(x) := \big((a+r)x + bx(x-1)\big)\,.$$

$$\frac{d}{dD}\log S(D) = \frac{1}{S(D)}\frac{d}{dD} S(D)\,,$$

using asymptotic arguments, together with the survival equation (7), it can be shown that the cell-survival curve tangent at the limit of low doses is given by

$$\begin{aligned}\frac{d}{dD}\log(S(D)\Big|_{D=0} &= -\frac{1}{z_F}\int_0^{\infty}(1-e^{-\kappa z})\, f_1(z)dz + \\ &+\frac{1}{z_F}\sum_{x_0\geq 1} C(x_0)\int_0^{\infty}\frac{e^{-\kappa z}}{x_0!}(\kappa z)^{x_0} f_1(z)dz\,.\end{aligned}$$

Further, the tangent to the cell-survival curve at asymptotically high dose is given by

$$\begin{aligned}\frac{d}{dD}\log(S(D)\Big|_{D=\infty} &= -\frac{1}{z_F}\int_0^{\infty}(1-e^{-\kappa z})\, f_1(z)dz + \\ &+\frac{1}{2z_F}\int_0^{\infty} e^{-\kappa z}\,\kappa z f_1(z)dz\,.\end{aligned}$$

Above two asymptotic limits show an extremely relevant feature of GSM^2 that is both low and high dose cell-survival asymptotic depends on the radiation quality as fully described by microdosimetric spectra.

The Repair-Misrepair Model

The RMR model considers that the amount of DSBs in the DNA, $U(t)$, is linearly proportional to the radiation dose rate; further DSBs evolve in lethal lesions, $L(t)$, while most breaks are successfully repaired with a first-order process. The model also includes the possibility of a misrepair as a second-order process, since it involves two broken DNA strands to form a chromosomal aberration.

These assumptions yield the following kinetic equations:

$$\begin{cases} \frac{d}{dt}U(t) &= -\rho U - \psi U^2\,, \\ \frac{d}{dt}L(t) &= (1-\phi)\rho U + \sigma\psi U^2\,. \end{cases} \quad (6)$$

where ρ is the rate at which DSBs are repaired ψ is the rate constant for second-order DSB interaction and ϕ is the fraction of simple successful repairs. The fraction of misrepairs that result in a lethal lesion is σ.

Consider also the MME given in equation (2), denoting by $\mathbb{E}$ the mean value of a random variable, we thus obtain

$$\begin{cases} \frac{d}{dt}\mathbb{E}[Y(t)] &= a\mathbb{E}[X(t)] + b\mathbb{E}[X(t)(X(t)-1)]\,, \\ \frac{d}{dt}\mathbb{E}[X(t)] &= -(a+r)\mathbb{E}[X(t)] - 2b\mathbb{E}[X(t)(X(t)-1)]\,. \end{cases} \quad (7)$$

Setting the parameters in the RMR driving equations (6) as

$$\psi = 2b\,, \quad \sigma = \frac{1}{2}\,, \quad \rho = a + r\,, \quad \phi = \frac{r}{a+r}\,,$$

then equations (6) become

$$\begin{cases} \frac{d}{dt}L(t) & = aU + bU^2\,, \\ \frac{d}{dt}U(t) & = -(a+r)U - 2bU^2\,. \end{cases} \quad (8)$$

Equations (7) and (8) have a similar form, but still not identical; in particular, (7) exhibits a dependence on a second order moment $\mathbb{E}[X(t)(X(t)-1)]$. Assuming a Poissonian distribution for the random variable X, we obtain that

$$\mathbb{E}[X(t)(X(t)-1)] = \mathbb{E}[X(t)]^2$$

so that, denoting further by $\bar{y}\ and\ \bar{x}$ the average number of lethal and sub-lethal lesions respectively, at last equation (7) becomes

$$\begin{cases} \frac{d}{dt}\bar{y}(t) & = b\bar{x}^2(t) + a\bar{x}(t)\,, \\ \frac{d}{dt}\bar{x}(t) & = -2b\bar{x}^2(t) - (a+r)\bar{x}(t)\,. \end{cases} \quad (9)$$

which are exactly the main kinetic equations of the RMR model given in equation (8).

Remark 2. Typically to solve an infinite system of interconnected moments equations, the so–called *mean–field* assumption is required; that is, we assume that

$$\mathbb{E}[X(t)(X(t)-1)] \sim \mathbb{E}[X(t)]^2\,.$$

A quick remark on the *mean–field assumption* is needed. In the case of x being large enough, we have that the following approximation holds true $\mathbb{E}[X(t)(X(t)-1)] \sim \mathbb{E}[X(t)]^2$; therefore, the *mean field assumption* means that $\mathbb{E}[X(t)(X(t)-1)] - \mathbb{E}[X(t)]^2 \sim 0$. Noticing that the last term is nothing but the variance and recalling that the variance for a random variable is null if and only if the random variable is in fact deterministic, if the *mean field assumption* is realistic, then the realized number of lesions does not differ much

from the mean value, and thus everything we need to know is the mean value. On the contrary if there are evidences that the mean value is not a realistic approximation for the realized number of lesions, the *mean–field assumption* must be considered unrealistic so that the knowledge of the full probability distribution is essential to have a complete understanding of the system.

Having cleared out the connection between the MME and the RMR, we aim now at explicitly solving equations (8). As reported in the Appendix A.2, the RMR can be solved explicitly to obtain

$$\begin{cases} U(t) & = \frac{(a+r)}{ce^{(a+r)t}-2b}\,, \\ L(t) & = \frac{1}{2}\left(\kappa D - U(t)\right) + \frac{a-r}{4b}\log\left(-\frac{2b\kappa D - e^{(a+r)t}(a+r+2b\kappa D)}{e^{(a+r)t}((a+r)}\right). \end{cases} \quad (10)$$

We can eventually calculate the long-time convergence toward the stationary solution of above equations (10) to be

$$\begin{aligned} \lim_{t\to\infty} U(t) & =: U_\infty = 0\,, \\ \lim_{t\to\infty} L(t) & =: \frac{1}{2}\kappa D + \frac{a-r}{4b}\log\left(1+\frac{2b\kappa D}{a+r}\right). \end{aligned} \quad (11)$$

The survival probability at time t is thus obtained computing the probability of having 0 lethal or sublethal lesions, under the assumption that they obey a Poissonian law. This implies, using equations (11),

$$S_{RMR}(D) = \exp[-L_\infty] = e^{-\frac{1}{2}\kappa D}\left(1+\kappa D\,\frac{2b}{a+r}\right)^{\frac{r-a}{4b}}. \quad (12)$$

Proceeding as above we can thus calculate the tangent of the logarithm of the cell–survival at low doses, i.e.

$$\frac{d}{dD}\log(S_{RMR}(D)\Big|_{D=0} = -\kappa\left(\frac{a}{a+r}\right). (13)$$

Similarly, at as the doses increases, the tangent of the log-survival becomes

$$\frac{d}{dD}\log(S_{RMR}(D)\Big|_{D=\infty} = -\frac{1}{2}\kappa. (14)$$

The GSM^2 in the Poisson initial damage case

As studied in details in (Cordoni, Missiaggia, Scifoni, et al. 2022), the initial damage–distribution according to the GSM^2 does not necessarily follow a Poisson distribution; nonetheless, in certain regimes, typically at both low-dose and low-LET, the initial distribution is significantly close to a Poisson law of average value κD. In such a case, the initial–damage distribution given in equation (5) simplifies to

$$p_0^X(x) = e^{-\kappa D}\frac{(\kappa D)^x}{x!}. (15)$$

Consider thus the MME (2) coupled with a Poisson initial condition (15). Such model will only exhibit non-Poissonian effects due to kinetic recombination of sub-lethal lesions.

Therefore, plugging-in the initial damage distribution (15) into the survival equation (7) we obtain

$$S_P(D) = e^{-\kappa D}\left(1 + \sum_{x_0=1}^{\infty}\frac{(\kappa D)^x}{x!}C(x_0)\right), (16)$$

It is worth stressing that, although the initial-damage distributed is Poissonian, the predicted cell-survival equation (16) includes some non-Poissonian terms coming from the coefficient b in the factor $C(x_0)$.

Again, we can study the tangent at high and low doses of the log-survival, to obtain

$$\begin{aligned} \frac{d}{dD}\log(S_P(D)\Big|_{D=0} &= -\kappa\left(\frac{a}{a+r}\right), \\ \frac{d}{dD}\log(S_P(D)\Big|_{D=\infty} &= -\frac{1}{2}\kappa. \end{aligned} \quad (17)$$

The Dirac GSM^2 in the $f_\nu(z) \approx \delta(z - \nu z_F)$ case

Recall that the initial damage distribution at a given dose D according to the GSM^2 is given by

$$p_0^X(x) := \sum_{\nu\geq 0} \int_0^\infty p_z^X(x|\kappa z) \frac{e^{-\frac{D}{z_F}}}{\nu!}\left(\frac{D}{z_F}\right)^\nu f_\nu(z)dz. \quad (18)$$

In order to simplify the GSM^2 initial damage distribution we can notice that the multi-event distribution $f_\nu(z)$ is sharply peaked around its average z_F; neglecting thus all the fluctuation around the mean value we can assume the following

$$f_\nu(z) \approx \delta(z - \nu z_F). \quad (19)$$

Equation (19) implies that the energy deposition by ν events equals νz_f, so that every events always deposits z_F.

Using assumption (19), the initial damage distribution thus (18) becomes

$$p_0^X(x) = \sum_{\nu\geq 0} e^{-\kappa\nu z_F} \frac{(\kappa\nu z_F)^x}{x!} \frac{e^{-\frac{D}{z_F}}}{\nu!}\left(\frac{D}{z_F}\right)^\nu. \quad (20)$$

Assumption (19) is clearly strong and not always valid. In fact, in the case of a low-LET radiation, whenever the number of registered microdosimetric events is close to the

theoretical average number of events $\frac{D}{z_F}$, it is true that f_ν is sharply peaked at νz_F . On the contrary, if the number of microdosimetric events is significantly smaller than $\frac{D}{z_F}$, the Dirac approximation (19) is not accurate, and the multi-event distribution could in principle be not well represented by the approximation (20). Nonetheless, it should be noticed that whenever $\nu \ll \frac{D}{z_F}$, the term

$$\frac{e^{-\frac{D}{z_F}}}{\nu!}\left(\frac{D}{z_F}\right)^{\nu}$$

appearing in the damage distribution (20) is small, so that the approximated damage distribution according to equation (20) can still be sufficiently close to the original damage distribution (18). The validity of such approximation will be investigated numerically in the next Section.

The distribution appearing in equation (20) is known in literature as *Neyman distribution* and it has been deeply studied and characterized in (Neyman 1939), in a purely theoretical context with no specific application.

The approximated initial damage distribution (20) can be thus inserted into the survival equation (7), to obtain

$$S_D(D) = p_0^X(0|D) + \frac{r}{a+r} p_0^X(1|D) + \sum_{x_0=2}^{\infty} p_0^X(x_0|D) C(x_0) \,, \quad (21)$$

where $p_0^X(x_0|D)$ is given by equation (20).

The tangent of the log-survival at low doses can be thus computed to be

$$\frac{d}{dD}\log(S(D)\Big|_{D=0} = -\frac{1}{z_F}(1-e^{-\kappa z_F}) + \\ +\frac{1}{z_F}\sum_{x\geq 1} C\,(x_0)\,\frac{e^{-\kappa z_F}}{x!}(\kappa z_F)^x\,,$$

whereas the tangent to the cell-survival curve at high dose is given by

$$\frac{d}{dD}\log(S(D)\Big|_{D=\infty} = -\frac{1}{z_F}\left(1-e^{-\kappa z_F}-\frac{1}{2}e^{-\kappa z_F}\kappa z_F\right).$$

Connection to the Multi–hit model

As briefly mentioned in (Cordoni, Missiaggia, Scifoni, et al. 2022), equation (7) can be seen as a microdosimetric generalization of the multi–hit model to account for damage dynamics and repair, as described by the term $C(x_0)$. In fact, choosing $C(x_0)$ to be either 0 or 1 respectively if x_0 is below or above a certain threshold, the standard formulation of a multi-hit model, (Zaider, Rossi, and Zaider 1996) can be recovered from the survival equation (7).

Notable enough, in (Vassiliev 2012), a non–Poissonian multi–hit model has been derived as follows. The survival curve is given by

$$S=\sum_{k=0}^{n-1} p\,(k)\,,\quad p(k)=e^{-a-ae^{-b}}\frac{b^k}{k!}B_k(ae^{-b})\,,\ (22)$$

being B_k the *Bell's polynomial*.

Recall that, under assumption (19), the initial damage (18) distribution is given by equation (20). Choosing

$$a=\frac{D}{z_F}\,,\quad b=\kappa z_F\,,$$

and using the relation

$$\sum_{i=0}^{\infty} \frac{i^k x^i}{i!} = e^x B_k(x)\,,$$

we can thus rewrite equation (20) as

$$p_0^X(x) = e^{-\frac{D}{z_F}(1-e^{-\kappa z_F})} \frac{\kappa z_F^x}{x!} B_k\left(\frac{D}{z_F} e^{-\kappa z_F}\right). \quad (23)$$

Distribution (23) thus provides a microdosimetric version of the distribution given in equation (20) and used in (Vassiliev 2012).

Comparing therefore the survival curve predicted by the *Multi-hit model* in (Vassiliev 2012), as given in equation (23), and the survival probability predicted by the Dirac GSM^2 in equation (7), it can be seen that the GSM^2 survival curve given in (23) provides a generalization to the survival given in (Vassiliev 2012) with the following added considerations:

- the parameters a and b given in (23) have a natural physical and mechanistic interpretation from microdosimetric arguments;

- the maximum number of hits is not a system parameter but it is naturally described by biological parameters of damage dynamics and repair;

- each term $p_0^X(x)$ is weighted by a term $C(x_0)$ that accounts for possible repair;

- a term accounting for initial lethal lesion formation is added.

Summary

Gathering results provided in this section, we get the following tangents for the log-survival curve, predicted including different levels of stochasticity, as collected in Table1.

In particular, notice first that considering the high and low–dose asymptotes in the GSM^{2}with assumption (19), we immediately recover the high and low–dose asymptotes of the Dirac GSM^2.

Further, in the case of a low–LET radiation, that is $\kappa z_F \ll 1$, considering the low and high dose asymptote for the log survival curve in the Dirac GSM^2 , we obtain

$$-\frac{1}{z_F}(1-e^{-\kappa z_F})+\frac{1}{z_F}\sum_{x_0\geq 1} C\,(x_0)\frac{e^{-\kappa z_F}}{x_0!}(\kappa z_F)^{x_0} \underset{\kappa z_F<<1}{\sim} -\kappa\left(\frac{a}{a+r}\right)$$

$$-\frac{1}{z_F}\left(1-e^{-\kappa z_F}-\frac{1}{2}e^{-\kappa z_F}\kappa z_F\right) \underset{\kappa z_F<<1}{\sim} -\frac{1}{2}\kappa$$

so that for a low–LET radiation quality, from both the Dirac GSM^2 and GSM^2 log survival curves we recover a Poissonian behavior.

Numerical results

The following numerical results of the theoretical predictions described in Section 2 will be shown. Microdosimetric spectra have been simulated using the TOPAS Monte Carlo toolkit (version 3.2.2 (Perl et al. 2012)) exploiting its microdosimetric extension, (Zhu et al. 2019); in particular, we employed the spherical tissue equivalent proportional chamber (TEPC) geometry available in the code. In particular, as previously done in (Missiaggia, Cordoni, et al. 2021), for numerical calculations a TEPC with a spherical active region equivalent to a

spherical tissue volume of 1 μm radius has been considered. This choice is mainly related to the authors' desire to stick to quantities usually measured experimentally with microdosimetry.

Four radiation fields have been simulated: (i) 80 MeV and (ii) 18.6 MeV proton undegraded "pristine" beams, (iii) 34 MeV/u carbon ion pristine beam, all impinging directly on the TEPC, and finally (iv) 70 MeV/u carbon ion impinging on a target phantom with 2 cm of water upstream the TEPC. The first three pencil beams radiation have been already used in (Missiaggia, Cordoni, et al. 2021), as exemplary cases of relatively low and high LET regimes with different particles, whereas the latter has been chosen, allowing a substantial build-up of fragments, in order to study a realistic mixed radiation field. It is in fact worth stressing that typically assumed approximations used in many existing radiobiological models fail in a strongly heterogeneous field, where instead GSM^2 is believed to provide an accurate prediction. Biological parameters considered are as follows: $a = 0.01$ [1/h], $b = 0.01$ [1/h] and $r = 2.9$ [1/h]. Such parameters have been fitted in (Missiaggia, Cordoni, et al. 2021) to predict the cell survival curve in the V79 cell line; different parameters can be chosen to predict cell survival in a different cell line. As regards the average yield of lesions per unit Gy, differently than previous works, the current paper implements a radiation quality-dependent parameter κ. In particular, following (Wang et al. 2018), the average yield of lesions K induced per unit Gy and per cell by certain ionizing radiation has been calculated via the fast Monte Carlo damage simulation (MCDS) software, (Wang et al. 2018) . The obtained parameters, according to Figure 1, are reported in Table 3.

Further, the average yield κ has been normalized to the volume of a spherical domain of 1 μm radius, as considered in this work. In particular, assuming that the cell nucleus has a radius of 5 μm, the resulting average yield κ in a 1 μm domain is obtained as

$$k\left[\frac{1}{Gy}\right] = K\left(\frac{1^3}{5^3}\right)\left[\frac{1}{Gy}\right]$$

where K is the average number of DNA damages per unit Gy per cell as calculated in (Wang et al. 2018).

In the present section, we analyze how the above-described radiation fields may affect cell survival prediction. In particular, different stochastic descriptions will be compared from a purely Poissonian description, as in the RMR, up to the general setting described by GSM^2 .

Figure 1 reports the multi-event microdosimetric distribution (3) compared to the Dirac approximation as described in equation (19) for a given dose $D = 1$ Gy, for the four radiation fields considered.

Panel (a) and (b), showing respectively the 18.6 MeV and 80 MeV proton beams, highlight that the Dirac approximation, despite having a clear Dirac comb-like behavior, well reproduces the first two moments of the multi-event distribution. Panel (c) shows how a slight underestimation in the Dirac approximation of the true variance appears in the 34 MeV/u carbon beam. Finally, for the mixed-field radiation beam illustrated in panel (d) a significant deviation of the Dirac approximated distribution emerges.

In Figure 2, the same study as Figure 1 is reported for a different dose of $D = 10$ Gy. In both the proton cases (panel (a) and (b)) the goodness of the Dirac approximation is confirmed;

in the 34 MeV/u carbon ion case (panel (c)) the approximated Dirac distribution is in better agreement compared to the previous case at $D = 1$ Gy. At last, the mixed field condition still shows clear discrepancies, especially in the second moment of the multi-event distribution.

Figure 3 shows the comparison of the sub-lethal damage distribution as described by GSM^2, the Dirac GSM^2, and the Poisson distribution, at low doses, i.e., $D = 1$ Gy. Panel (a) and (b) report respectively the case of higher LET and lower LET protons, showing how the three distributions are similar, with a slight discrepancy in the Poisson case. For the case of pencil beam carbon ion (panel (c)), it can be seen how the Dirac GSM^2 and the GSM^2 damage distributions are identical, whereas the Poisson case is significantly different. Regarding the mixed field case, its damage distribution slightly differs from the GSM^2 one, as it can be seen in the main peak, and they both are significantly different in the Poisson density.

Figure 4 reports the same analysis as Figure 3 in the case of $D = 10$ Gy; the same comments of the previous figure hold also in the higher dose scenario, with no significant differences to be reported. Nonetheless, a clear difference between the damage distribution for GSM^2 and the Dirac GSM^2 in both the carbon ions beams.

Figure 5 illustrates the cell-survival curve prediction by the four different models in the four radiation fields. In panel (a), for the case of 18.6 MeV protons, an agreement emerges for all the models at low doses. As the doses increase, the behavior of the models starts to differ, with the RMR model giving a lower survival probability, followed by the Poisson GSM^2 and at last the Dirac GSM^2 and the GSM^2 predict a higher survival fraction. Panel (b)

Discussion and Conclusions

In Section 2 we have studied four different models, namely the RMR, the Poisson GSM^2 , the Dirac GSM^2, and the GSM^2 , of increasing generality with respect to the stochastic effects included in them. In particular, the RMR assumes a purely Poissonian initial damage distribution as well as Poissonian dynamics. In fact, the kinematic equations are purely deterministic, and they describe the time evolution of the average values of damages. Also, the Poisson-GSM^2 neglects non–Poissonian stochastic fluctuations in the initial damage distribution but Poissonian effects of repair and cluster death are included via the MME (2).

The Dirac-GSM^2 is instead a purely non-Poissonian model in the sense that both initial damage distribution and the dynamical equation include non-Poissonian effects of both overkilling and clustered death. The Dirac GSM^2 can be thus regarded as ~~a~~ faster implementation of the GSM^2 since the initial damage distribution calculation is less demanding numerically compared to the original formulation of the GSM^2. Nonetheless, the second moment of the microdosimetric distribution z_D is not included in the model so fluctuations in the energy deposition are not fully described. It can be thus expected that for monoenergetic undegraded beams such approximation is valid as the microdosimetric distribution is in fact sharply peaked at the average value z_F.

At last, GSM^2 is the most general model of the four considered when it comes to including several levels of stochasticity. GSM^2 accounts in fact for non-Poissonian effects at both initial and dynamical levels. Further, all the variations in the energy deposition at the micrometer scale are included in the model via a full microdosimetric treatment. Such

generality is believed to be relevant and leads to significantly different results, especially in mixed radiation fields.

All of the above considerations of the different levels of stochasticity taken into account in the four different models are summarized in Table 2 and depicted in Figure 6.

In Section 2 we have further seen how the low and high dose log-survival tangent of the four models may be significantly different and, most important by, how different information on the radiation quality is included in the predicted cell survival curve. Results on this topic are summarized in Table 1.

From Table 1 it emerges how both the RMR and the Poisson GSM^2 predict cell survival with the same tangent at both low and high doses. Nonetheless, it is worth stressing that the two cell survival curves may have different curvatures due to non-Poissonian effects included in the GSM^2 via the MME (2). In addition, both asymptotes of the low and high dose do not depend on the radiation quality. Regarding the biological parameters, the low dose limits depend on the linear rates a and r, and the rate of decrease of the log-survival is proportional to the rate at which a sub-lethal lesion dies normalized to the overall linear rates, i.e., $\frac{a}{a+r}$. Also, the quadratic rate given by b does not appear in the low-dose asymptote since it gives a term of order 2, which is negligible compared to the linear terms. Regarding the high-dose asymptotics, it depends only on the average damage yield parameter κ since at infinite dose only initial damage matters with no significant role played by dynamics.

The Dirac GSM^2 has both high and low–dose log-survival tangents that depend on the radiation quality only via the first microdosimetric moment z_F. This is expected since ~~the~~

assumption (19) neglects all the fluctuations in the energy deposition. The low-dose limit, in this case, is more complex than in the Poisson case with an explicit dependence on the number of damages, given by the summation over x_0 weighted for the repair weighting function $C(x_0)$. The high–dose limit depends as before on the average damage yield parameter κ with no repairs involved; differently again from the Poisson case, the asymptote is more complex, and the radiation quality affects the limit via the first moment z_F. As regard to this point, as already commented in (Vassiliev et al. 2019), *fluence–average values*, e.g. y_F and z_F, can be measured more reliably than dose–average values, e.g. y_D and z_D, (Inaniwa et al. 2013). This fact implies that a model based on z_F, for instance, the *Dirac* GSM^2, is more robust to experimental uncertainties than classical radiobiological models based on z_D, such as the MKM and its variants.

At last, GSM^2 shows low and high–dose limit that depends on the full microdosimetric description of the radiation quality besides a general description of the DNA–damage complexity. As before, in the high-dose case, only initial damage is relevant.

As shown in Section 2.5, the asymptotes of the models are strictly related in the sense that, starting from the more general GSM^2 , we can recover other models' asymptotes by making specific assumptions. In particular, if we assume a Dirac-like microdosimetric initial distribution in the GSM^2 we recover, as expected, the tangents as predicted by the Dirac GSM^2 . Further, for a low–LET radiation, meaning that $\kappa z_F \ll 1$, the Dirac GSM^2 gives the same asymptotes as the Poisson GSM^2 and the RMR.

From Figures 1–2, it can be seen how the multi–event distribution computed under the Dirac assumption (25) is a Dirac comb-like version of the full multi–event distribution f_n. In

both cases of the proton pencil beam, the Dirac multi–event distribution well reproduces both the mean and variance of the multi–event distribution f_n, especially as the dose increases the two distributions are extremely similar. In the case of the carbon pencil beam, a larger discrepancy compared to the proton case can be seen, even if still the Dirac distribution is able to capture the main features of the distribution f_n. In particular, both distributions share a similar description of the no-hit probability, a fact that is extremely relevant in capturing overkilling effects of high–LET radiations. Nonetheless, in the high dose case, some discrepancies emerge as the two distributions appear to have a slightly different variance. The mixed radiation field, on the contrary, highlights how a radiation quality description only via the microdosimetric first moment is inadequate. There are in fact clear discrepancies between the two distributions. Therefore, Figures 2–1 suggest that although the Dirac assumption (19) completely neglects energy deposition fluctuations, it is still able to provide an accurate description of the energy deposition at the micrometer scale. This is coherent since, in a purely monoenergetic pristine beam, the microdosimetric distribution is sharply peaked around its average. Therefore, since the Dirac–like multi–event distribution neglects the fluctuations in the energy deposition but still includes the fluctuations in the number of registered events, a good agreement between the Dirac multi–event and the full microdosimetric multi–event distribution emerges. On the contrary, more complex radiation fields such as the exemplary mixed field considered, are not very well described by the Dirac multi–event distribution. In such cases, the microdosimetric distributions are not simply peaked around the mean values since contributions from different ions at different energies are extremely relevant. Therefore, in

these fields, a more complex and consistent radiation quality description, like the one included in GSM^2 , appears to be necessary.

The multi–event distribution directly affects DNA damage distribution. As noted above, since the Dirac multi–event distribution well describes the multi–event microdosimetric distribution in the monoenergetic case, we immediately obtain that the initial damage distribution as described by GSM^2 and the Dirac GSM^2 is in good agreement. Further, as expected, the proton pencil beam cases are also well described by a Poisson law, with the higher LET proton's initial damage distribution predicted by GSM^2 and the Dirac GSM^2 being slightly different from a Poisson distribution. A similar analysis has already emerged in (Missiaggia, Cordoni, et al. 2021). The Dirac GSM^2 and the GSM^2 also give a similar initial damage distribution in the carbon pristine beam, both being extremely different from a Poisson distribution. Relevant enough, the GSM^2 initial damage distribution shows a clear bi-modal distribution with a significant probability of inducing no damages, as typical in the high–LET case. Finally, previously noted differences in the mixed field case are still evident in the DNA damage distribution.

At last, the above discrepancies and analogies emerge in the cell–survival curve prediction. The lower–LET case shows an overall agreement in the survival fraction prediction by all four models. In this sense, GSM^2 recovers a Poissonian description of the DNA damage formation and evolution. In the case of higher LET protons, it can be seen that GSM^2 , the Dirac GSM^2, and the Poisson GSM^2 predict the same cell survival curve, whereas the RMR gives a significantly lower cell survival curve. Since the three versions of the GSM^2 share the same dynamical description, the previously noted similarity in the initial damage

distribution is reflected in the cell survival computation. Therefore, since the RMR and the Poisson GSM^2 predict different survival curves, it can be deduced that recombination of lesions leading to cell death is relevant already in higher LET protons. Further, it is worth stressing that, even if the RMR and the Poisson GSM^2 have the same high and low–dose asymptotes, the predicted cell–survival curves can differ. The cell survival curve in the carbon pristine beam shows instead how a Poissonian initial damage distribution leads to different results compared to the GSM^2 and the Dirac–GSM^2 . Both RMR and the Poisson–GSM^2 give the same cell–survival curve which is clearly different from the one predicted by the Dirac GSM^2 and GSM^2. Important enough, the cell–survival curve given by the Dirac GSM^2 and the GSM^2 presents in the high LET cases a clear linear trend, a feature that emerges consistently in radiobiological experiments with high LET ions. On the contrary, the RMR and the Poisson GSM^2 predict a cell survival curve where a quadratic non-linear term lowers the cell survival curve at higher doses. Further, slight differences between the GSM^2 and the Dirac GSM^2 emerge in the cell survival curve prediction at high doses. Finally, coherently with the previous analysis, differences emerge in the cell survival predicted by the four models in the mixed radiation field. This might suggest that in a general, complex radiation field various effects may contribute to cell death. It can be seen how the RMR predicts the lower cell survival, bounded above by the Poisson GSM^2 , followed by a higher cell survival curve predicted by the Dirac GSM^2 and at last the GSM^2 shows the higher survival probability. Moreover, the slope is increasing, with the GSM^2 giving an almost linear behavior. Regarding the difference between the cell survival curve predicted by the Dirac GSM^2 and by the GSM^2 , the following considerations can further be made. As extensively noted above, the Dirac GSM^2 describes the radiation

quality via the fluence–average parameter z_F. For monoenergetic beams, such a value well represents the whole microdosimetric distribution. Therefore, the cell survival prediction made by GSM^2 , which instead considers the whole microdosimetric distribution, coincides with the prediction made by the Dirac GSM^2 . On the contrary, in mixed radiation fields z_F is no longer significant to describe the whole distribution. This in fact emerges as the GSM^2 and the Dirac GSM^2 predict different cell survival curves.

We thus presented how deeply investigating the different levels of stochasticity included in a radiation damage process, induced by a general type of radiation field, provides important insights into how such levels affect cell killing in different cases. At the same time, the present results emphasize on one side the consistency of GSM^2 with other models when decreasing its level of generality, and on the other side how GSM^2 can be a comprehensive tool allowing a larger mechanistic significance to the adopted parameters, strictly bound to microdosimetric arguments.

Declaration of Interest

No potential conflict of interest was reported by the author(s).

Acknowledgments

This work has been partially supported by the INFN-CNS5 projects Microbe_IT and FRIDA.

Notes on contributors

Francesco G. Cordoni, Ph.D., is a *tenure track assistant professor* at the University of Trento, Department of Civil, Environmental and Mechanical Engineering, Trento, Italy.

Marta Missiaggia, Ph.D., is a *Research Fellow* at the Museo Storico della Fisica e Centro Studi e Ricerche Enrico Fermi, Rome, Italy.

Chiara La Tessa, Ph.D., is an *Associate Professor* at the University of Trento, Department of Physics, Trento, Italy.

Emanuele Scifoni, Ph.D., is a *Senior Researcher* at the Trento Institute for Fundamental Physics and Applications (TIFPA) of the Istituto Nazionale di Fisica Nucleare (INFN), Trento, Italy.

Albright, Norman. 1989. "A Markov Formulation of the Repair-Misrepair Model of Cell Survival." *Radiation research* 118(1): 1–20.

Bellinzona, Valentina Elettra et al. 2021. "Linking Microdosimetric Measurements to Biological Effectiveness in Ion Beam Therapy: A Review of Theoretical Aspects of MKM and Other Models." *Frontiers in Physics* 8: 623.

Bernal, Mario A et al. 2015. "Track Structure Modeling in Liquid Water: A Review of the Geant4-DNA Very Low Energy Extension of the Geant4 Monte Carlo Simulation Toolkit." *Physica Medica* 31(8): 861–74.

Brenner, David J. 1990. "Track Structure, Lesion Development, and Cell Survival." *Radiation Research* 124(1s): S29–37.

Charlton, DE and Nikjoo, H and Humm, JL. 1989. "Calculation of Initial Yields of Single-and Double-Strand Breaks in Cell Nuclei from Electrons, Protons and Alpha Particles." *International journal of radiation biology 56*(1), 1-19.

Chen, Yizheng et al. 2017. "A Modified Microdosimetric Kinetic Model for Relative Biological Effectiveness Calculation." *Physics in Medicine & Biology* 63(1): 015008.

Cordoni, F, M Missiaggia, A Attili, et al. 2021. "Generalized Stochastic Microdosimetric Model: The Main Formulation." *Physical Review E* 103(1): 012412.

Cordoni, F, M Missiaggia, E Scifoni, and C La Tessa. 2022. "Cell Survival Computation via the Generalized Stochastic Microdosimetric Model (GSM^2) - Part I: The Theoretical Framework." *Radiation Research,* 197.3: 218-232.

Curtis, Stanley B. 1986. “Lethal and Potentially Lethal Lesions Induced by Radiation—a Unified Repair Model.” *Radiation research* 106(2): 252–70.

Dingfelder, Michael. 2012. “Track-Structure Simulations for Charged Particles.” *Health physics 103*(5), 590-595.

Friedland, Werner, Michael Dingfelder, Pavel Kundrát, and Peter Jacob. 2011. “Track Structures, DNA Targets and Radiation Effects in the Biophysical Monte Carlo Simulation Code PARTRAC.” *Mutation Research/Fundamental and Molecular Mechanisms of Mutagenesis* 711(1–2): 28–40.

Friedrich, T, M Durante, and M Scholz. 2015. “Simulation of DSB Yield for High LET Radiation.” *Radiation protection dosimetry* 166(1–4): 61–65.

Friedrich, Thomas et al. 2012. “Calculation of the Biological Effects of Ion Beams Based on the Microscopic Spatial Damage Distribution Pattern.” *International journal of radiation biology* 88(1–2): 103–7.

Goodhead, DT and Leenhouts, HP and Paretzke, HG and Terrissol, M and Nikjoo, H and Blaauboer, R. 1994. “Track Structure Approaches to the Interpretation of Radiation Effects on DNA.” *Radiation Protection Dosimetry 52*(1-4), 217-223.

Hawkins, Roland B. 1994. “A Statistical Theory of Cell Killing by Radiation of Varying Linear Energy Transfer.” *Radiation research* 140(3): 366–74.

———. 2003. “A Microdosimetric-Kinetic Model for the Effect of Non-Poisson Distribution of Lethal Lesions on the Variation of RBE with LET.” *Radiation research* 160(1): 61–69.

———. 2018. “A Microdosimetric-Kinetic Model of Cell Killing by Irradiation from Permanently Incorporated Radionuclides.” *Radiation research* 189(1): 104–16.

Inaniwa, Taku et al. 2013. “Effects of Dose-Delivery Time Structure on Biological Effectiveness for Therapeutic Carbon-Ion Beams Evaluated with Microdosimetric Kinetic Model.” *Radiation research* 180(1): 44–59.

Incerti, Sebastien et al. 2016. “Review of Geant4-DNA Applications for Micro and Nanoscale Simulations.” *Physica Medica* 32(10): 1187–1200.

———. 2018. “Geant4-DNA Example Applications for Track Structure Simulations in Liquid Water: A Report from the Geant4-DNA Project.” *Medical physics* 45(8): e722–39.

Kase, Yuki et al. 2006. “Microdosimetric Measurements and Estimation of Human Cell Survival for Heavy-Ion Beams.” *Radiation research* 166(4): 629–38.

Kellerer, Albrecht M, and Harald H Rossi. 1978. “A Generalized Formulation of Dual Radiation Action.” *Radiation research* 75(3): 471–88.

Kyriakou, Ioanna et al. 2017. “Microdosimetry of Electrons in Liquid Water Using the Low-Energy Models of Geant4.” *Journal of Applied Physics* 122(2): 024303.

———. 2021. “Review of the Geant4-Dna Simulation Toolkit for Radiobiological Applications at the Cellular and Dna Level.” *Cancers* 14(1): 35.

McMahon, Stephen Joseph. 2018. “The Linear Quadratic Model: Usage, Interpretation and Challenges.” *Physics in Medicine & Biology* 64(1): 01TR01.

Missiaggia, M, E Pierobon, et al. 2021. “A Novel Hybrid Microdosimeter for Radiation Field Characterization Based on TEPC Detector and LGADs Tracker: A Feasibility Study.” *Frontiers in Physics, 8, 578444*.

Missiaggia, M, F Cordoni, E Scifoni, and C La Tessa. 2021. “Cell Survival Computation via the Generalized Stochastic Microdosimetric Model (GSM^2) - Part II: Numerical Results via Monte Carlo Simulated Spectra.” *submitted*.

Neyman, J. 1939. “On a New Class of" Contagious" Distributions Applicable in Entomology and Bacteriology.” *Ann. Math. Statistics* 10: 35–57.

Nikjoo H., S. Uehara W.E. Wilson M. Hoshi M. D.T. Goodhead. 1998. “Track Structure in Radiation Biology: Theory and Applications.” *International journal of radiation biology 73*(4), 355-364.

Nomiya, Takuma. 2013. “Discussions on Target Theory: Past and Present.” *Journal of radiation research* 54(6): 1161–63.

Paretzke, Herwig G. 1987. “Radiation Track Structure.” *Kinetics of Non-homogeneous Processes* 89.

Perl, Joseph et al. 2012. “TOPAS: An Innovative Proton Monte Carlo Platform for Research and Clinical Applications.” *Medical physics* 39(11): 6818–37.

Plante, Ianik. 2011. “A Monte–Carlo Step-by-Step Simulation Code of the Non-Homogeneous Chemistry of the Radiolysis of Water and Aqueous Solutions. Part I: Theoretical Framework and Implementation.” *Radiation and environmental biophysics* 50(3): 389–403.

Plante, Ianik, Floriane Poignant, and Tony Slaba. 2021. “Track Structure Components: Characterizing Energy Deposited in Spherical Cells from Direct and Peripheral HZE Ion Hits.” *Life* 11(11): 1112.

Rossi, HH, and M Zaider. 1988. “Saturation in Dual Radiation Action.” In *Quantitative Mathematical Models in Radiation Biology*, Springer, 111–18.

Sato, Tatsuhiko, and Yoshiya Furusawa. 2012. “Cell Survival Fraction Estimation Based on the Probability Densities of Domain and Cell Nucleus Specific Energies Using Improved Microdosimetric Kinetic Models.” *Radiation research* 178(4): 341–56.

Scholz, M, AM Kellerer, W Kraft-Weyrather, and G Kraft. 1997. “Computation of Cell Survival in Heavy Ion Beams for Therapy.” *Radiation and environmental biophysics* 36(1): 59–66.

Schuemann, J et al. 2019. “TOPAS-NBio: An Extension to the TOPAS Simulation Toolkit for Cellular and Sub-Cellular Radiobiology.” *Radiation research* 191(2): 125–38.

Tobias, Cornelius A. 1980. “The Repair-Misrepair Model of Cell Survival.”

———. 1985. “The Repair-Misrepair Model in Radiobiology: Comparison to Other Models.” *Radiation Research* 104(2s): S77–95.

Vassiliev, Oleg N. 2012. “Formulation of the Multi-Hit Model with a Non-Poisson Distribution of Hits.” *International Journal of Radiation Oncology* Biology* Physics* 83(4): 1311–16.

———. 2017. “Microdosimetry. Elements of Stochastic Transport Theory.” In *Monte Carlo Methods for Radiation Transport*, Springer, 195–223.

———. 2019. “Systematic Microdosimetric Data for Protons of Therapeutic Energies Calculated with Geant4-DNA.” *Physics in Medicine & Biology* 64(21): 215018.

Wälzlein, C, M Krämer, E Scifoni, and M Durante. 2014. “Advancing the Modeling in Particle Therapy: From Track Structure to Treatment Planning.” *Applied Radiation and Isotopes* 83: 171–76.

Wang, Wenjing et al. 2018. “Modelling of Cellular Survival Following Radiation-Induced DNA Double-Strand Breaks.” *Scientific Reports* 8(1): 1–12.

Zaider, M and Brenner, DJ and Wilson, WE. 1983. “The Applications of Track Calculations to Radiobiology I. Monte Carlo Simulation of Proton Tracks.” *Radiation research 95*(2), 231-247.

Zaider, M, By Harald H Rossi, and Marco Zaider. 1996. *Microdosimetry and Its Applications*. Springer.

Zhao, Lei, Dong Mi, Bei Hu, and Yeqing Sun. 2015. “A Generalized Target Theory and Its Applications.” *Scientific reports* 5(1): 1–11.

Zhao, Lei, Dong Mi, and Yeqing Sun. 2017. “A Novel Multitarget Model of Radiation-Induced Cell Killing Based on the Gaussian Distribution.” *Journal of Theoretical Biology* 420: 135–43.

Zhu, Hongyu et al. 2019. "The Microdosimetric Extension in TOPAS: Development and Comparison with Published Data." *Physics in Medicine & Biology* 64(14): 145004.

Appendix

A.1 Some further results on the GSM^2

Taking into account further the specific form for the initial damage as given in equation (5), it has been showed in (Cordoni, Missiaggia, Scifoni, et al. 2021) that, via classical properties of the Laplace transform, the survival curve can be written as

$$S(D) = \exp\left[-\frac{D}{z_F}\int_0^\infty (1-e^{-\kappa z})\, f_1(z)dz\right]\left(1+\sum_{k=1}^\infty \left(\frac{D}{z_F}\right)^k G_k(M)\right),$$

with

$$G_k(M) := \sum_{x_0=k}^\infty \sum_{i=1}^{x_0}\sum_{j=1}^{i} \frac{(-1)^i(-1)^j}{(i-j)!(j-k)!}\frac{(-\kappa)^{x_0}}{x_0!} C(x_0) M^{i-k} B_{x_0,k}\left(M_1,\dots,M_{x_0-k+1}\right),$$

with $B_{x,l}(M_1,\dots,M_{x-l+1})$ the *Bell's polynomial* defined as

$$B_{x,l}(M_1,\dots,M_{x-l+1}) := \sum \frac{x!}{j_1!\dots j_{x-l+1}!}(M_1)^{j_1}\dots(M_{x-l+1})^{j_{x-l+1}},$$

where the sum ranges over multiple indexes such that

$$\begin{aligned} &j_1 + j_2 + \cdots + j_{x-l+1} = l\,, \\ &j_1 + 2j_2 + \cdots + (x-l+1)j_{x-l+1} = x\,. \end{aligned}$$

We can give a probabilistic interpretation to the terms above; in fact, in the survival in equation (7) the terms $p_0^X(x_0|D)$ gives the probability that the domain suffers x_0 lesions.

This probability is weighted by a term $C(x_0)$ that represents the probability that x_0 sub–lethal lesions recover in order to let the domain survive.

From equation (8) we obtain the log–survival curve

$$\log S(D) = \\ = \left[-\frac{D}{z_F}\int_0^\infty (1-e^{-\kappa z})\, f_1(z)dz\right] + \log\left(1+\sum_{k=1}^\infty \left(\frac{D}{z_F}\right)^k G_k(M)\right).$$

A.2 Explicit derivation of the solution to the RMR model

The present Section is devoted to an explicit solution of the dynamical equations (11) as described by the RMR. In particular, we have that

$$\frac{d}{dt}U(t) = -(a+r)U - 2bU^2\,, \quad U(0) = \kappa D\,. \quad (31)$$

Previous equation (31) is known in literature as Bernoulli equation. In order to solve it, the transformation $u = \frac{1}{U}$ can be applied, so that explicit calculation lead to the following differential equation

$$\dot{u}(t) = (a+r)u(t) + 2b\,.$$

This last equation is a linear equation in u, so that explicit solution is given by

$$u(t) = ce^{(a+r)t} - \frac{2b}{(a+r)}.$$

Coming back to the original equation we obtain

$$U(t) = \frac{(a+r)}{ce^{(a+r)t} - 2b}, \quad (32)$$

with

$$c := \frac{(a+r)}{\kappa D} + 2b\,.$$

We can therefore substitute U into the equation for L in (11) to obtain

$$\begin{aligned}\frac{d}{dt}L(t) &= aU + bU^2 = \\ &= -\frac{1}{2}\big(-(a+r)U(t) - 2bU^2(t)\big) + \frac{a-r}{2}U(t) = \\ &= -\frac{1}{2}\dot{U}(t) + \frac{a-r}{2}U(t)\,,\end{aligned}$$

so that after integration we obtain

$$L(t) \quad = \tfrac{1}{2}\big(\kappa D - U(t)\big) + \tfrac{a-r}{4b}\log\Big(-\tfrac{2b\kappa D - e^{(a+r)t}(a+r+2b\kappa D)}{e^{(a+r)t}((a+r)}\Big)\,. \quad (33)$$

	Low-dose tangent	High dose tangent
RMR	$-\kappa(\frac{a}{a+r})$	$-\frac{1}{2}\kappa$
Poisson GSM^2	$-\kappa(\frac{a}{a+r})$	$-\frac{1}{2}\kappa$
Dirac GSM^2	$-\frac{1}{z_F}\left(1-e^{-\kappa z_F}\right)+$ $+\frac{1}{z_F}\sum_{x_0\geq 1} C(x_0)\frac{e^{-\kappa z_F}}{x_0!}\left(\kappa z_F\right)^x$	$-\frac{1}{z_F}\left(1-e^{-\kappa z_F}-\frac{1}{2}e^{-\kappa z_F}\kappa z_F\right)$
GSM^2	$-\frac{1}{z_F}\int_0^\infty\left(1-e^{-\kappa z}\right)f_1(z)dz+$ $+\frac{1}{z_F}\sum_{x_0\geq 1} C(x_0)\int_0^\infty\frac{e^{-\kappa z}}{x_0!}\left(\kappa z\right)^x f_1(z)dz$	$-\frac{1}{z_F}\int_0^\infty\left(1-e^{-\kappa z}\right)f_1(z)dz+$ $+\frac{1}{2z_F}\int_0^\infty e^{-\kappa z}\kappa z f_1(z)dz$

Table 1: Low and high dose log-survival tangent limits for the RMR, Poisson GSM^2, Dirac GSM^2 and GSM^2.

	Non Poissonian effects		Radiation quality dependence	
	Initial damage	Dynamical	First moment	Microdosimetric distribution
RMR	×	×	×	×
Poisson GSM^2	×	√	×	×
Dirac GSM^2	√	√	√	×
GSM^2	√	√	√	√

Table 2: Levels of non–Poissonian effects included into the models, both for the initial damage distribution or for kinetics equations. Radiation quality dependence of the high and low-dose log-survival asymptotic, either including the first moment of the microdosimetric distribution or the whole microdosimetric spectra.

Ion	p 18.6 MeV	p 80 MeV	C 34 MeV	C mixed field
Average yield per Gy per cell K [1/Gy]	50	50	90	100
Average yield per Gy per domain κ [1/Gy]	0.4	0.4	0.72	0.8

Table 3: considered average number of radio-induced damages for the four radiation fields considered in the present work.

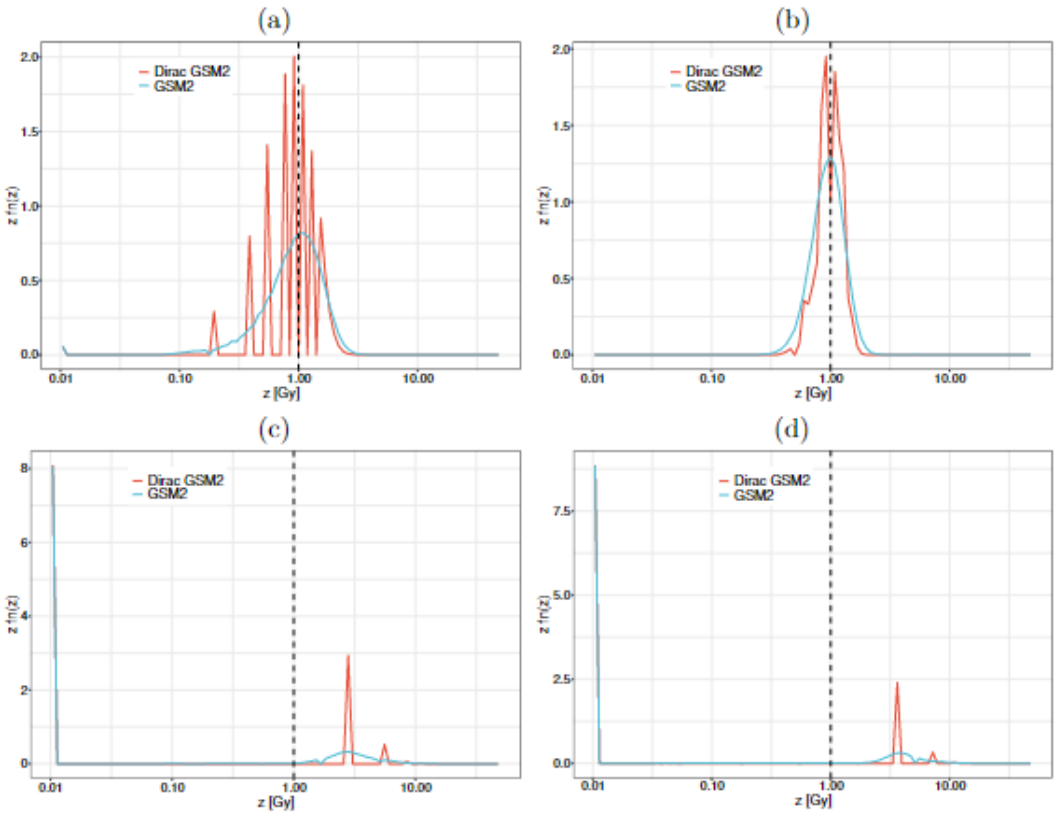

Figure 1: Comparison between the multi–event microdosimetric distribution fn, as given in equation (3), (blue line) compared to the Dirac approximation multi-event distribution (red line), at D = 1 Gy. Vertical black dotted line denotes the average of the distribution,

corresponding to D = 1 Gy. Panels refer to (a) protons at 18.6 MeV (top left panel), (b) protons at 80 MeV (top right panel), (c) carbon ions at 24 MeV (bottom left panel) and (d) carbon ions after 2 cm of water (bottom right panel).

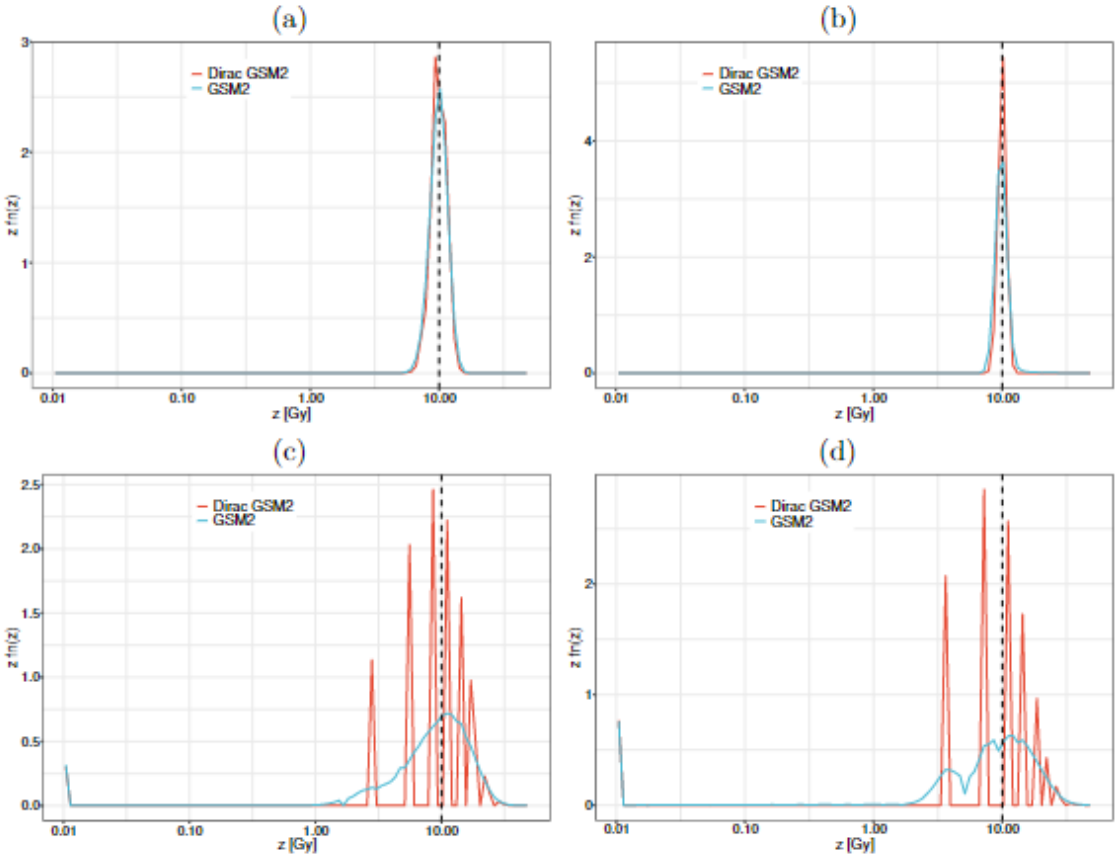

Figure 2: Comparison between the multi–event microdosimetric distribution fn, as given in equation (3), (blue line) compared to the Dirac approximation multi-event distribution (red line), at D = 10 Gy. Vertical black dotted line denotes the average of the distribution, corresponding to D = 10 Gy. Panels refer to (a) protons at 18.6 MeV (top left panel), (b) protons at 80 MeV (top right panel), (c) carbon ions at 24 MeV (bottom left panel) and (d) carbon ions after 2 cm of water (bottom right panel).

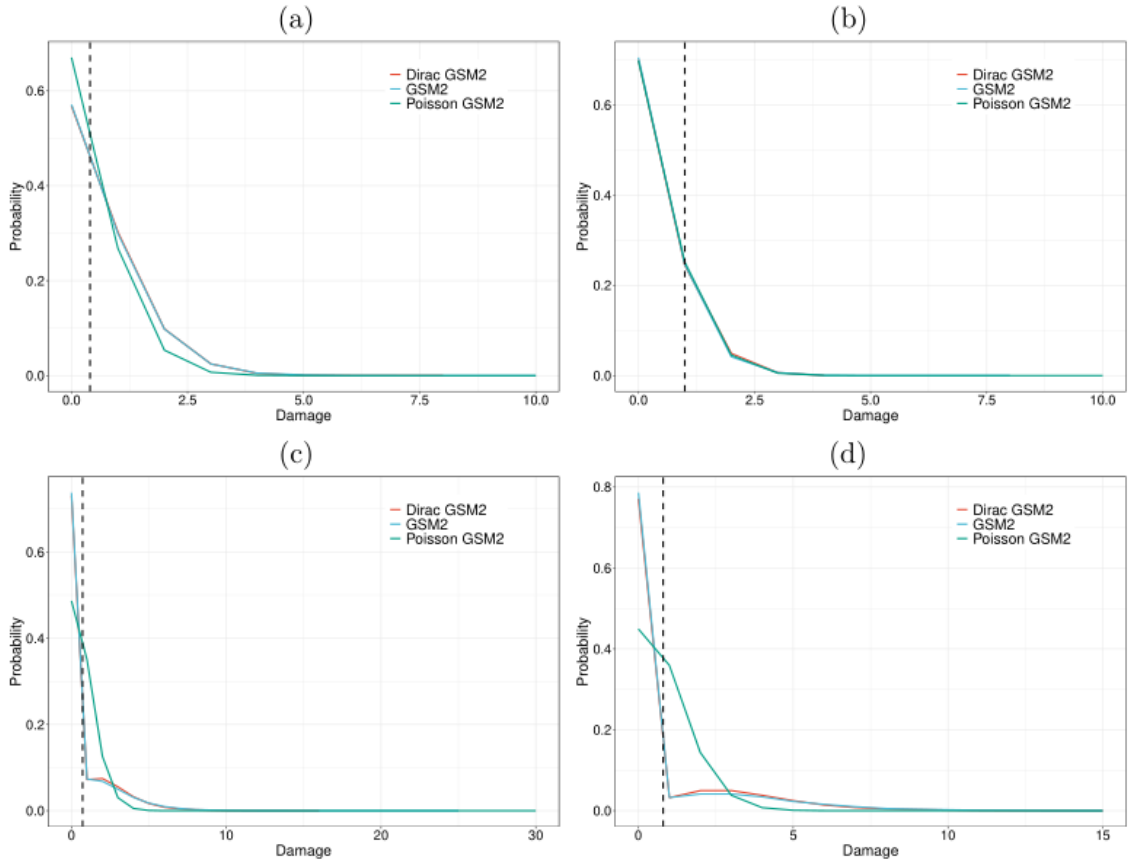

Figure 3: Comparison between the sub–lethal damage distribution, as given in equation (5), (blue line) compared to the Dirac approximation sub–lethal distribution equation (29) (red line), and to the Poisson distribution (green line), at D = 1 Gy. Vertical black dotted line denotes the average of the distributions. Panels refer to (i) protons at 18.6 MeV (top left panel), (ii) protons at 80 MeV (top right panel), carbon ions at 24 MeV (bottom left panel) and (iv) carbon ions after 2 cm of water (bottom right panel).

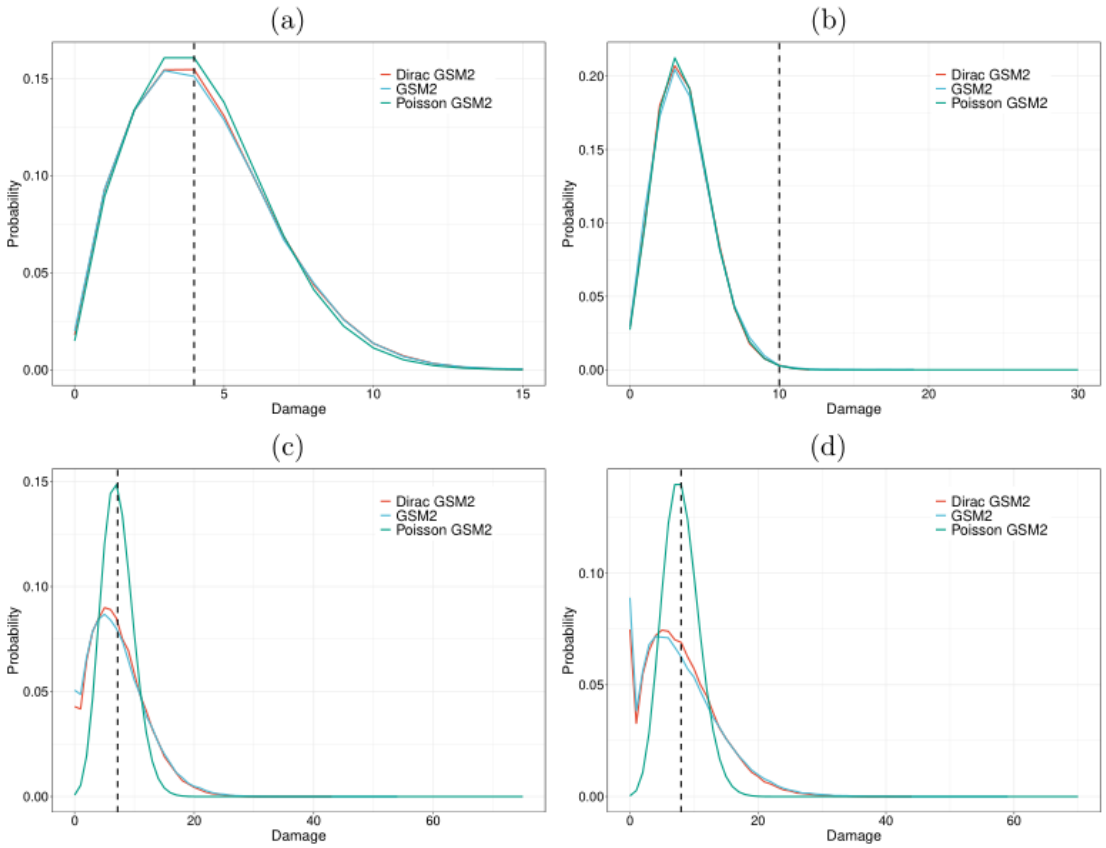

Figure 4: Comparison between the sub–lethal damage distribution, as given in equation (5), (blue line) compared to the Dirac approximation sub–lethal distribution equation (29) (red line), and to the Poisson distribution (green line), at D = 10 Gy. Vertical black dotted line denotes the average of the distributions. Panels refer to (a) protons at 18.6 MeV (top left panel), (b) protons at 80 MeV (top right panel), (c) carbon ions at 24 MeV (bottom left panel) and (d) carbon ions after 2 cm of water (bottom right panel).

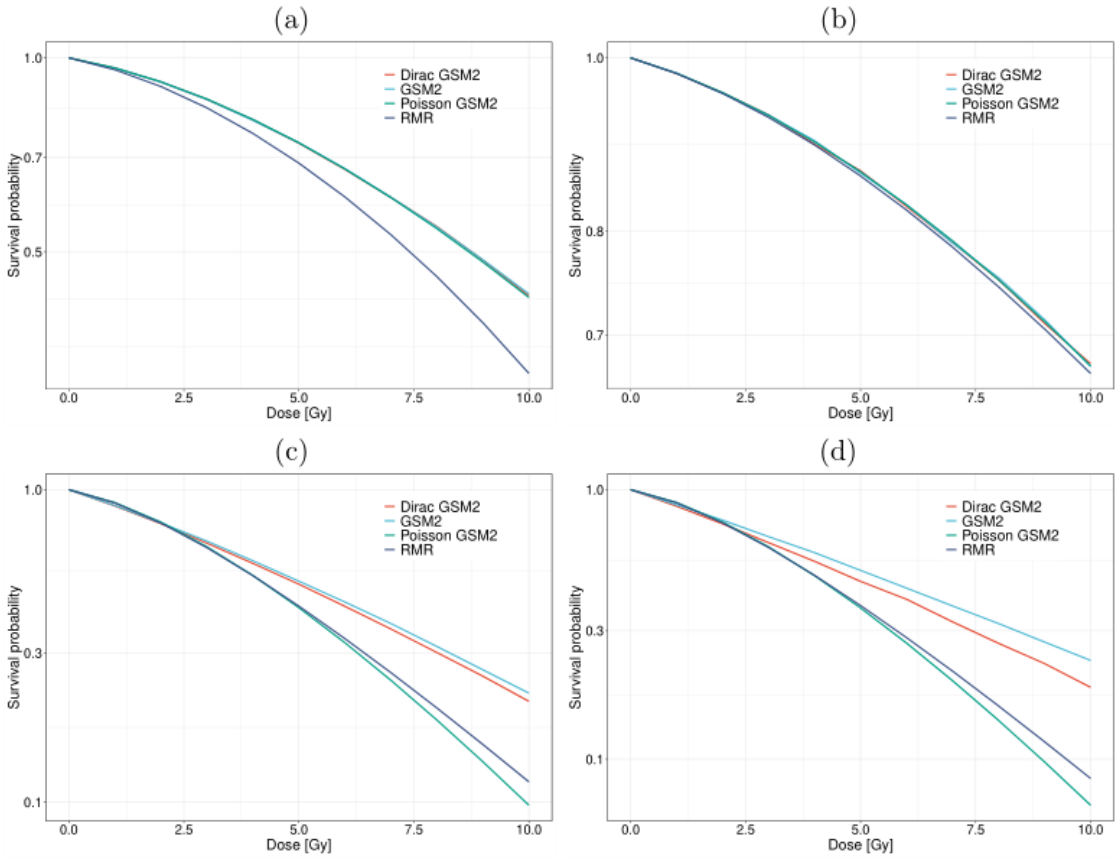

Figure 5: Survival curves for the GSM^2 (blue line), the Dirac GSM^2 (red line), Poisson GSM^2 (green line) and the RMR (purple line), at different doses. Panels refer to (a) protons at 18.6 MeV (top left panel), (b) protons at 80 MeV (top right panel), (c) carbon ions at 24 MeV (bottom left panel) and (d) carbon ions after 2 cm of water (bottom right panel).

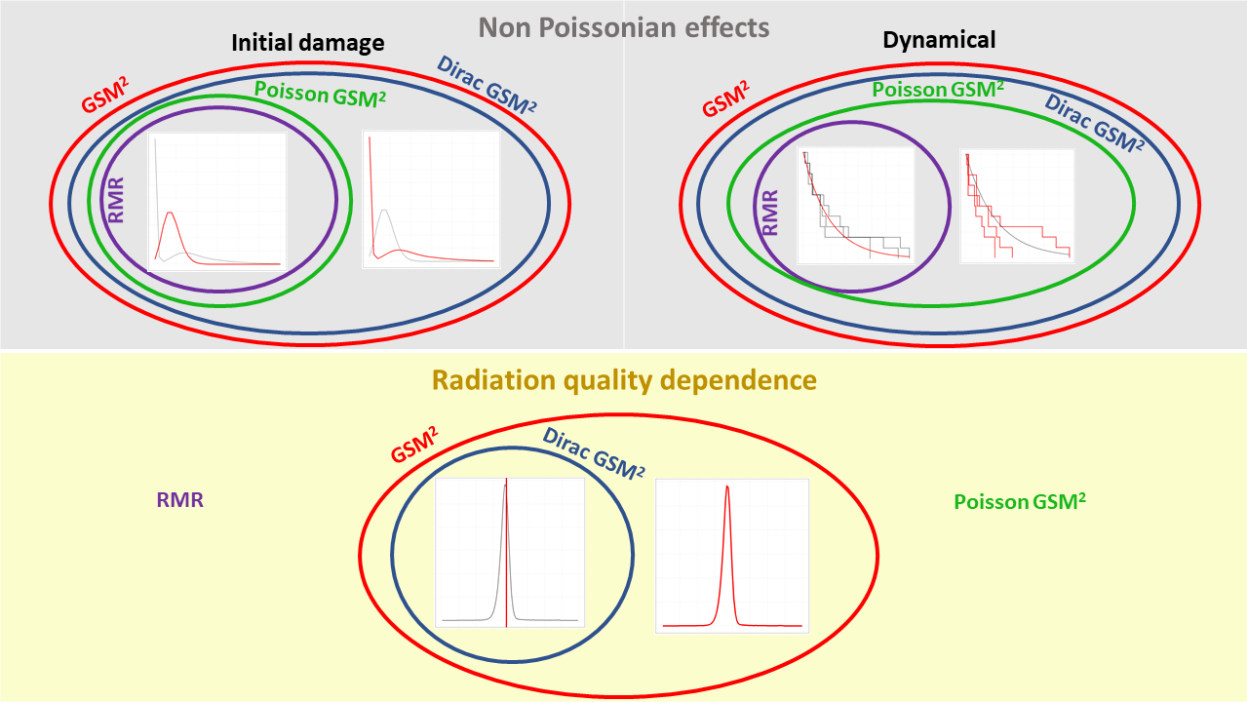

Figure 6: Levels of non–Poissonian effects included into the models, both for the initial damage distribution or for kinetics equations. Radiation quality dependence of the high and low-dose log-survival asymptotic, either including the first moment of the microdosimetric distribution or the whole microdosimetric spectra.